"The interpretation of results is the art of turning data into insights, transforming the complex into the understandable."

– Arunima Sen

3

Impact on CP measurement sensitivity in light of scalar Non-Standard Interaction

The measurement of the CP (Charge-Parity) phase in neutrino physics is a crucial endeavor that seeks to unravel one of the most profound mysteries of the universe. CP violation, the asymmetry between the behavior of particles and their antiparticles under the combined operations of charge conjugation (C) and parity inversion (P), holds the key to understanding why there is a prevalence of matter over antimatter in the universe. Neutrinos, elusive and electrically neutral particles, offer a unique avenue to investigate CP violation due to their oscillation behavior. Experiments involving neutrino beams and detectors, such as long-baseline neutrino experiments and neutrino oscillation studies, aim to precisely measure the CP phase, which introduces a distortion in the oscillation pattern. This phase has the potential to hold the answers to why the cosmos is dominated by matter and holds implications for our comprehension of fundamental symmetries and the evolution of the early universe. Accurate CP phase measurements represent a critical step in advancing our understanding of neutrinos and their role in shaping the fundamental building blocks of the universe.

3.1 Scalar NSI & δ_{CP} measurement

The well-established framework of neutrino oscillations [1] has yielded one of the initial unequivocal indications of physics that goes beyond the Standard Model (BSM). An expansion of the Standard Model (SM) becomes necessary to account for neutrino oscillations, which confirm the non-zero masses of neutrinos, despite the SM's remarkable success. As we venture beyond the SM to elucidate neutrino mixing and its related phenomena, numerous BSM models propose supplementary interactions collectively termed non-standard interactions (NSI). These NSIs might have ramifications on the creation, travel, and detection of neutrinos across diverse neutrino experiments, emphasizing the need for a comprehensive comprehension of their potential effects. The analysis of scalar NSIs has gained prominence as a burgeoning field for investigating novel interactions within various neutrino experiments. In this paper, we delve into the consequences of a general scalar NSI on neutrino mixing. Significantly, we undertake a comprehensive examination of how it influences the sensitivity to CP-violation in the context of the proposed long-baseline neutrino experiment DUNE [81].

Recent investigations have delved into the exploration of potential non-standard connections between neutrinos and a scalar field [7, 145, 146]. This form of scalar interaction emerges as a corrective element to the neutrino mass term [11], bringing about distinct phenomenological implications compared to vector-mediated NSIs. A range of studies have been conducted to examine the ramifications of these scalar NSI components while considering astrophysical, cosmological, terrestrial, and space-based experimental constraints [11, 147]. The existence of scalar NSIs has been invoked to elucidate the observed Borexino data [7]. Additionally, given that scalar NSIs augment the neutrino mass matrix, their influence on neutrino mass models is both captivating and promising. These scalar connections might also affect the measurement of diverse neutrino oscillation parameters in a variety of neutrino oscillation experiments. Notably, the effects of scalar NSIs are directly proportional to the surrounding matter density, rendering long-baseline neutrino experiments particularly apt for probing these effects.

In this investigation, we have undertaken an impartial analysis of the implications stemming from scalar NSI parameters on long-baseline neutrino experiments, using DUNE as a focal case. This study represents one of the pioneering comprehensive inquiries into the effects of such scalar NSIs specifically within the context of DUNE. Our findings highlight the potential of scalar NSIs to exert a considerable influence on the accuracy of δ_{CP} phase measurements at DUNE. Our approach begins by formulating scalar NSIs as a matrix, allowing us to scrutinize their effects element by element. Detailed explication of the scalar NSI formalism is extensively provided in the ensuing

sections. For the purpose of this study, we have focused on diagonal NSI parameters. Notably, the impact of scalar NSIs tends to be most prominent around oscillation maxima. Furthermore, we identify various instances of degeneracies in the determination of δ_{CP} in the presence of scalar NSI components.

Continuing our investigation, we proceed to examine the potential influence of NSIs on the measurement of CP-violation at DUNE. Our analysis underscores the considerable impact of diagonal scalar NSI parameters on DUNE's measurements. Specifically, we demonstrate that selected values of scalar NSI parameters can lead to an enhancement in the experiment's sensitivity. Additionally, we explore DUNE's capacity for precision CP-violation measurements within the context of scalar NSIs. Our study establishes that the experiment's efficacy in constraining δ_{CP} is significantly altered when these NSI parameters are taken into account. Depending on the specific values of scalar NSI parameters, we observe scenarios where the experiment's precision measurement capability is diminished, while other parameter values enhance this capacity. Consequently, the precise determination of these NSI parameters is of utmost importance for achieving robust δ_{CP} sensitivities at DUNE.

3.2 Simulation details

The occurrences of neutrino oscillations have significantly contributed to enhancing our comprehension of diverse neutrino attributes through various neutrino experiments. Particularly in long baseline (LBL) neutrino experiments, the predominant neutrino oscillation channels of interest encompass $\nu_\mu \to \nu_e$ (appearance) and $\nu_\mu \to \nu_\mu$ (disappearance) probability transitions. Our investigation centers on examining the impacts of scalar NSIs on these neutrino oscillation probabilities.

We have conducted an examination of the repercussions introduced by the diagonal scalar NSI components, specifically η_{ee}, $\eta_{\mu\mu}$, and $\eta_{\tau\tau}$, on the probabilities of neutrino oscillation. The values assigned to the oscillation parameters employed throughout this analysis can be found in table 3.1. The Hamiltonian, when affected by scalar NSIs, also exhibits dependence on the absolute neutrino masses (equation 2.11). For our computations, we have taken the value of m_1 to be 10^{-5} eV, which subsequently helps in the determination of m_2 and m_3 through the values of Δm^2_{21} and Δm^2_{31}. Notably, the analysis consistently assumes the normal ordering of neutrino masses as the true hierarchy. To incorporate the effects of scalar NSIs, we have introduced modifications to the NuOscProbExact package [16]. This package, implemented in Python, serves as a generator for neutrino oscillation probabilities. It employs SU(2) and SU(3) expansions

of evolution operators to precisely compute probabilities for both two-flavour and three-flavour neutrino oscillations in scenarios governed by time-independent Hamiltonians. In the context of scalar NSIs, we have adjusted the Hamiltonian using the equation 2.11. Our computations incorporate three distinct definitions of M_{eff}, as delineated in equations 2.16, 2.17, and 2.18, serving as test cases.

Parameters	True Values
θ_{12}	34.51°
θ_{13}	8.44°
θ_{23}	47°
δ_{CP}	$-\pi/2$
Δm^2_{21}	$7.56 \times 10^{-5}\ eV^2$
Δm^2_{31}	$2.55 \times 10^{-3}\ eV^2$

TABLE 3.1: The benchmark values of oscillation parameters used in the analysis [25].

3.3 Effects on the oscillation probabilities

The phenomenon of neutrino oscillations has played a pivotal role in advancing our understanding of various nuanced properties associated with neutrinos, and these insights have been gleaned from a range of diverse neutrino experiments. In the context of long baseline (LBL) neutrino experiments, which involve the study of neutrino behavior over substantial distances, the most pertinent and scrutinized oscillation channels are the $\nu_\mu \rightarrow \nu_e$ (appearance) and $\nu_\mu \rightarrow \nu_\mu$ (disappearance) probability transitions. In these LBL experiments, neutrinos emitted as one type - often ν_μ - transform into a different type, such as ν_e, over the course of their journey. Similarly, neutrinos of a particular type, such as ν_μ, can also maintain their identity as they travel, known as disappearance. These oscillation probabilities provide a critical lens through which to investigate the characteristics and behaviors of neutrinos.

In this study, we have undertaken a comprehensive exploration of how scalar non-standard interactions (NSIs) influence these fundamental neutrino oscillation probabilities. By investigating the potential impact of scalar NSIs on these oscillation channels, we aim to unravel potential deviations from the expected oscillation patterns dictated solely by the Standard Model of particle physics. This investigation not only expands our comprehension of neutrino behavior but also has implications for our broader understanding of the fundamental nature of particles and their interactions beyond the Standard Model. We see that,

- The impact of diagonal scalar NSIs on the oscillation probabilities of DUNE is notably substantial, particularly around the oscillation peaks. For the η_{ee} element, positive values lead to an enhancement of probabilities around the oscillation maxima, while negative values result in probability suppression.

- In the top-right panel and the bottom panel of figure 3.1, the effects of $\eta_{\mu\mu}$ (case II, eq.2.17) and $\eta_{\tau\tau}$ (case III, eq.2.18) on the appearance probability $P_{\mu e}$ at DUNE are depicted. Positive values of $\eta_{\mu\mu}$ shift the oscillation peaks towards higher energies, while negative values shift them towards lower energies, accompanied by a general suppression in probabilities.

- The behavior of probabilities concerning $\eta_{\tau\tau}$ follows a similar pattern - probabilities are suppressed (enhanced) with increasing positive (negative) non-zero values of $\eta_{\tau\tau}$.

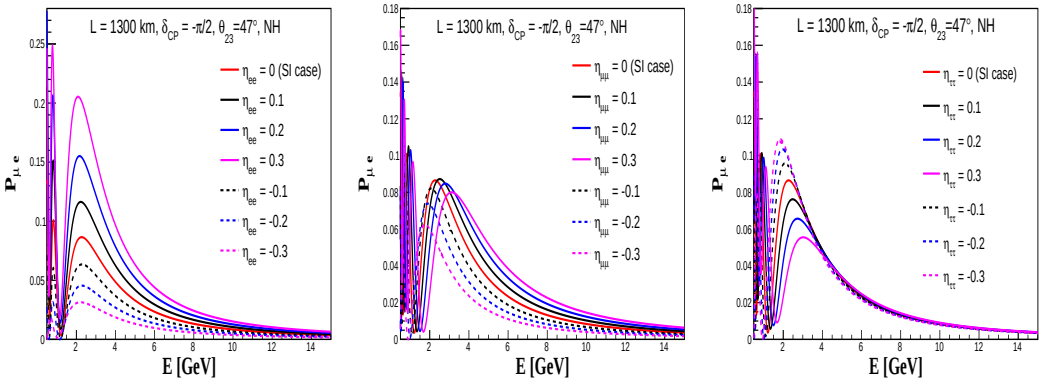

FIGURE 3.1: The effects of η_{ee} (top-left panel), $\eta_{\mu\mu}$ (top-right panel), and $\eta_{\tau\tau}$ (bottom panel) on $P_{\mu e}$ for δ_{CP} = -π/2, θ_{23} = 47° and NH. In every subfigure, the red-solid curve is for the SI case and the other solid (dashed) curves are for positive (negative) non-zero values of $\eta_{\alpha\beta}$.

Figure 3.2 illustrates the profound influence of scalar NSIs on the appearance probability ($P_{\mu e}$) concerning its dependency on the CP-violating phase (δ_{CP}). The parameters chosen for this demonstration encompass a neutrino beam energy of E = 2.5 GeV, a θ_{23} angle of 47 degrees, and the normal hierarchy (NH) as the underlying hierarchy assumption.

Within this visual representation, the distinct impact of scalar NSIs is showcased across three panels. In the top-left panel, we observe the variation in the appearance probability due to the η_{ee} element, while the top-right panel illustrates the effects induced by $\eta_{\mu\mu}$. In the bottom panel, the consequences of $\eta_{\tau\tau}$ are depicted. Each of these panels investigates a range of chosen values spanning from -0.3 to 0.3 for the respective scalar NSI elements.

Throughout figure 3.2, a consistent reference point is maintained through the red-solid line, which represents the scenario where scalar NSIs are absent ($\eta_{\alpha\beta} = 0$), commonly referred to as the Standard Interaction (SI) case. This benchmark line serves as the baseline against which the diverse effects of scalar NSIs can be clearly discerned, elucidating the intricate interplay between these interactions and the CP-violating phase (δ_{CP}) within the context of neutrino appearance probabilities. We note that,

- The behavior of the appearance probability ($P_{\mu e}$) in response to variations in the η_{ee} element is characterized by a discernible pattern. As the values of η_{ee} become increasingly positive, the appearance probability is enhanced, whereas increasing negative values of η_{ee} lead to its suppression.

- In the presence of non-zero $\eta_{\mu\mu}$, the probabilities exhibit a consistent trend of suppression. Irrespective of whether the chosen values for $\eta_{\mu\mu}$ are positive or negative, a reduction in probabilities is observed.

- For the element $\eta_{\tau\tau}$, positive values correspond to a suppression of probabilities, while negative values result in their enhancement.

- An intriguing observation involves the presence of degeneracies within the probability curves for certain values of $\eta_{\alpha\beta}$. This phenomenon introduces intricacies into the probability patterns, potentially influencing the experiment's ability to precisely measure the CP-violating phase (δ_{CP}).

- These intricate patterns underscore the complex interplay between scalar NSIs and neutrino appearance probabilities, highlighting the multifaceted nature of neutrino oscillations and their response to non-standard interactions.

The considerable reliance of the probability on both δ_{CP} and $\eta_{\alpha\beta}$ introduces an intriguing aspect, prompting us to delve deeper into the data to unveil noteworthy regions of interest. In order to facilitate a comparative and quantitative assessment of the influence exerted by scalar NSIs on the probability, we introduce the parameter $\Delta P_{\alpha\beta}$, defined as:

$$\Delta P_{\alpha\beta} = P_{\alpha\beta}(\text{with SNSI}) - P_{\alpha\beta}(\text{without SNSI}). \tag{3.1}$$

The parameter, $\Delta P_{\alpha\beta}$, serves as a metric for gauging the shift in probability brought about by the presence of scalar NSIs in contrast to scenarios where scalar NSI effects are absent. By quantifying these variations, we can effectively characterize the magnitude and direction of alterations in the probability due to the introduction of scalar NSI.

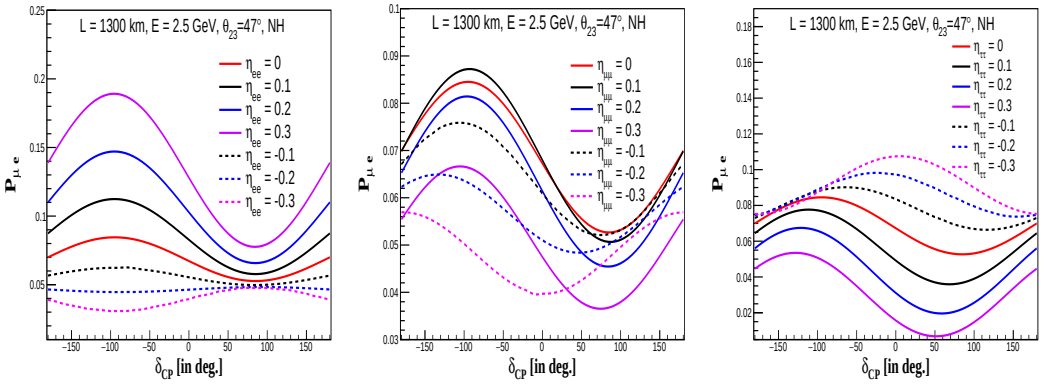

FIGURE 3.2: The effects of η_{ee} (top-left panel), $\eta_{\mu\mu}$ (top-right panel), and $\eta_{\tau\tau}$ (bottom panel) on $P_{\mu e}$ as a function of δ_{CP} at $\theta_{23} = 47°$ and $E = 2.5$ GeV. In every panel, the red-solid line is for $\eta_{\alpha\beta} = 0$ (i.e, the SI case), and other solid (dashed) coloured lines are for positive (negative) non-zero values of $\eta_{\alpha\beta}$.

In figure 3.3, we conduct a comprehensive examination by scanning the values of $\Delta P_{\alpha\beta}$ across an extensive parameter space as a function of $\eta_{\alpha\beta}$ and δ_{CP}. Throughout this analysis, we maintain a consistent neutrino beam energy of E = 2.5 GeV, θ_{23} angle at 47°, and assume the normal hierarchy (NH) to be the true hierarchy configuration. In each of the plots of the figure 3.3, $\eta_{\alpha\beta}$ parameters undergo variation within the range of -0.3 to 0.3, capturing a broad spectrum of potential values for these scalar NSI components. Concurrently, the CP-violating phase δ_{CP} is explored across the entire 3σ range from -π to π, enabling a comprehensive exploration of its impact on the parameter $\Delta P_{\alpha\beta}$. This intricate and systematic investigation provides valuable insights into how changes in both $\eta_{\alpha\beta}$ and δ_{CP} interplay to alter the observed $\Delta P_{\alpha\beta}$, contributing to a deeper understanding of the effects of scalar NSI on the neutrino appearance probabilities. We note that,

- An interesting observation emerges when considering the range of true δ_{CP} values spanning from -π to 0. In this context, the presence of a non-zero η_{ee} is shown to have a substantial influence on the probability, as depicted in the top-left panel.

- The impact of $\eta_{\mu\mu}$ becomes apparent in the upper-right panel, although the magnitude of this effect appears to be somewhat milder compared to that of η_{ee}.

- The lower panel, on the other hand, highlights a particularly significant impact due to $\eta_{\tau\tau}$ within a more constrained δ_{CP} range of [-π/3, π]. This scalar NSI component's effect on the probability is markedly significant in this region.

- These observations underscore the intricate relationship between δ_{CP} and the various scalar NSI elements, elucidating the distinct roles that different NSI components play in shaping the behavior of neutrino appearance probabilities across specific ranges of the CP-violating phase.

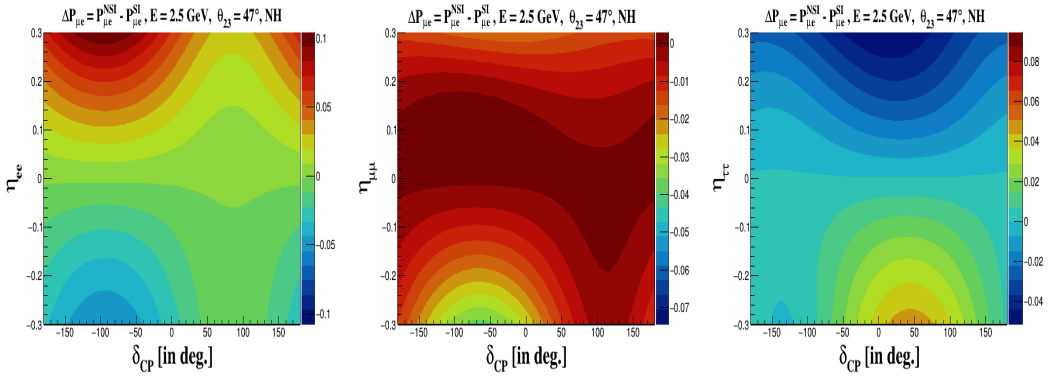

FIGURE 3.3: The variation of $\Delta P_{\alpha\beta}$ on $\eta_{\alpha\beta}$ - δ_{CP} plane. We show the results for η_{ee} (top-left panel), $\eta_{\mu\mu}$ (top-right panel) and $\eta_{\tau\tau}$ (bottom panel).

3.4 Impact on the detector sensitivity

We employed the General Long Baseline Experiment Simulator (GLoBES) [138, 148, 149], a dedicated tool renowned for its ability to simulate neutrino experiments, particularly those involving long-baseline neutrino oscillation studies. The details of GLoBES and its various modules are discussed in appendix B. In the context of this study, we focused on a liquid-argon detector configuration, mirroring the specifications of DUNE with a baseline extending to 1300 km. To replicate the experimental conditions, we considered a simulation duration of 5 years for both neutrino and antineutrino modes, resulting in a cumulative exposure of 35 $\times$ 10^{22} kt-POT-yr. Our analysis incorporates the comprehensive combination of appearance and disappearance channels, maximizing the data's discriminatory power. For normalization purposes, we adopted a 2% (5%) uncertainty for the signal in neutrino (antineutrino) mode. Concurrently, the background was subject to a 10% normalization error in both modes. The energy resolution was defined for muons (R_μ) and electrons (R_e), set at $20\%/\sqrt{E}$ and $15\%/\sqrt{E}$, respectively. Moreover, an energy calibration error of 5% was taken into account for both neutrino and antineutrino modes. Drawing from the Technical Design Report (TDR) of DUNE [142], we established our foundation for addressing background considerations and defining the systematic uncertainties inherent in our simulations. Further specifics regarding the experimental setup and the associated systematic uncertainties

are meticulously cataloged within table 2.2, encapsulating the comprehensive framework underlying our simulation endeavors.

The central objective of our analysis revolves around delineating the impact of diagonal scalar NSI elements on CP-violation measurements conducted at DUNE. Our exploration extends to encompass both the assessment of CP-violation and the precision of CP measurements within the experiment's context while accommodating the presence of scalar NSIs. The efficacy of an experiment in discerning between CP-conserving and CP-violating instances of δ_{CP} stands as a pivotal indicator of its CP sensitivity. Throughout our analysis, we have consistently adopted the normal hierarchy (NH) as the true hierarchy, and unless explicitly stated, the higher octant (HO) represents a true θ_{23} of 47°. By accounting for systematic uncertainties through a process of marginalization, we ensure a comprehensive assessment of the effects under consideration. It is worth noting that the specific parameter values utilized in our analysis are extracted from table 3.1, unless otherwise specified, thus reinforcing the consistency and rigor of our approach.

3.4.1 Effects on the event rates

To probe DUNE's sensitivity in the presence of scalar NSIs, we begin by investigating the event rates detected by the DUNE detector. Illustrated in figure 3.4, these binned events are portrayed against the reconstructed neutrino energy. The parameter values employed to generate the event plots are succinctly outlined in table 3.1. The solid-red histogram serves to depict the event rate in the absence of scalar NSIs, establishing a baseline for comparison. For scenarios involving positive and negative scalar NSI elements, specifically η_{ee}, $\eta_{\mu\mu}$, and $\eta_{\tau\tau}$, both solid and dashed histograms delineate binned events. Importantly, the behavior of these binned events resonates well with the predicted probabilities. In instances where positive η_{ee} values are introduced, the event count increases across each bin relative to the 'no scalar NSI' scenario. Conversely, for negative η_{ee} values, a decrease in event counts is observed within each bin. Considering $\eta_{\mu\mu}$ and $\eta_{\tau\tau}$, the impact is more intricate. Positive (negative) $\eta_{\mu\mu}$ values lead to a shift of the event plot peaks towards higher (lower) energy bins. Additionally, positive (negative) $\eta_{\mu\mu}$ values result in heightened (reduced) event counts around the oscillation maxima, whereas positive (negative) $\eta_{\tau\tau}$ values yield a decrease (increase) in event counts within the same oscillation maxima range. This comprehensive analysis of event rates and their dependence on scalar NSIs effectively mirrors the corresponding probability trends, thus establishing a cohesive connection between the physical phenomena and their observed consequences in the experimental context.

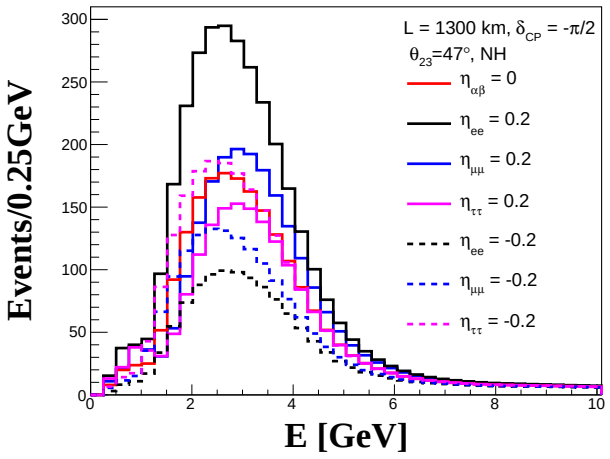

FIGURE 3.4: The binned event rates as a function of the neutrino energy for different choices of $\eta_{\alpha\beta}$. The results shown here are for δ_{CP} = -$\pi/2$, $\theta_{23} = 47°$ and NH.

3.4.2 NSI parameter sensitivity

Displayed in figure 3.5, our analysis delves into DUNE's discerning power concerning $\eta_{\alpha\beta}$. Here, we assume the true $\eta_{\alpha\beta}$ values to be 0.1 (left panel) and -0.1 (right panel), while systematically varying the test values of $\eta_{\alpha\beta}$ across the range of -0.3 to 0.3.

Regardless of the chosen true $\eta_{\alpha\beta}$ value, DUNE's proficiency in constraining η_{ee} appears to be relatively subdued when contrasted with its capabilities towards $\eta_{\mu\mu}$ and $\eta_{\tau\tau}$. This observation underscores the distinct sensitivities exhibited by DUNE when confronted with scalar NSI elements of different diagonal components.

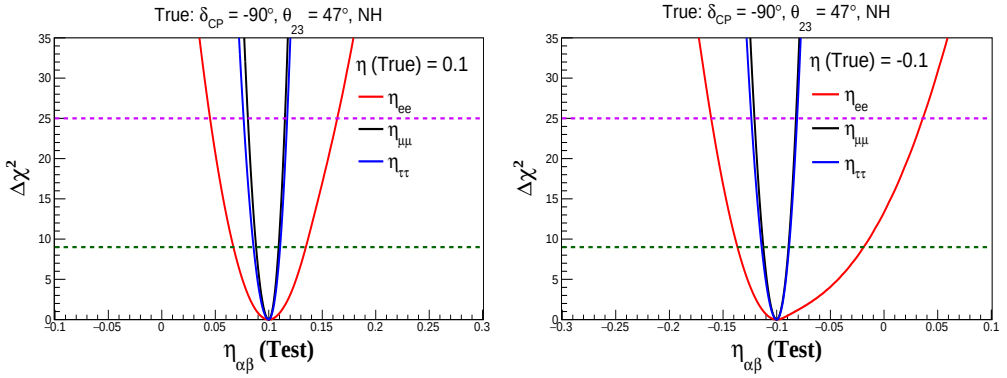

FIGURE 3.5: The sensitivity of DUNE to true $\eta_{\alpha\beta} = 0.1$ (left panel) and true $\eta_{\alpha\beta}$ = -0.1 (right panel) at true δ_{CP} = -$\pi/2$ and true $\theta_{23} = 47°$. In both of the plots, the red-solid curve is for η_{ee}, the black-solid curve is for $\eta_{\mu\mu}$, and the blue-solid curve is for $\eta_{\tau\tau}$.

3.4.3 Effects on the CPV sensitivity

Illustrated in figure 3.6, our study ventures into the realm of CP-violation (CPV) sensitivity as wielded by DUNE amidst the presence of scalar NSI elements η_{ee}, $\eta_{\mu\mu}$, and $\eta_{\tau\tau}$. This investigation adheres to a specific methodology wherein we exclude test δ_{CP} values that uphold CP conservation. Consequently, the true value for δ_{CP} is methodically varied within the permissible span of [-π,π].

To ascertain DUNE's CPV sensitivity, we calculate the minimal value of $\Delta\chi^2$ through a process of marginalization spanning the allowed 3σ region for θ_{23} and Δm^2_{31}. Our approach to quantifying CPV sensitivity is encapsulated by the formula:

$$\Delta\chi^2_{\rm CPV}\ (\delta^{\rm true}_{\rm CP}) = \min\ \left[\chi^2\ (\delta^{\rm true}_{CP}, \delta^{\rm test}_{CP} = 0),\ \chi^2(\delta^{\rm true}_{CP}, \delta^{\rm test}_{CP} = \pm\pi)\right]. \tag{3.2}$$

This metric enables us to gauge DUNE's capability in detecting CP-violating tendencies while factoring in the influence of scalar NSIs and diverse test values of δ_{CP}. In this context, we have additionally employed a marginalization technique over the test values of $\eta_{\alpha\beta}$ for the various NSI scenarios under consideration.

Within each of the three panels presented in figure 3.6, distinctive visual representations unfold. The red-solid curve elegantly captures the scenario without scalar NSIs, effectively forming the baseline comparison. Meanwhile, the black and blue lines (represented as solid-dashed) depict instances with non-zero positive and negative values of the selected scalar NSI parameters. For enhanced clarity, the horizontal dashed lines colored in magenta and green intersect the graph. These lines correspondingly signify the 5σ and 3σ confidence levels (CL) within the parameter space, facilitating an intuitive comprehension of the statistical significance associated with different outcomes. We observe that,

- In the top-left panel of figure 3.6, it becomes evident that the CPV sensitivity of the experiment experiences significant enhancement (suppression) in the presence of positive (negative) η_{ee} values.
- When considering negative η_{ee} values, the CPV sensitivity falls below the 3σ confidence level, indicating that such scenarios can undermine DUNE's ability to measure CPV.
- Moving to the top-right panel of the same figure, we observe that positive $\eta_{\mu\mu}$ values don't considerably alter DUNE's sensitivity in the negative half-plane of δ_{CP}.

- Conversely, positive $\eta_{\mu\mu}$ values diminish the CPV sensitivity compared to the baseline case in the positive half-plane of δ_{CP}. For chosen negative non-zero $\eta_{\mu\mu}$ values, the CPV sensitivity experiences significant suppression relative to the baseline sensitivity without scalar NSI.

- It's noteworthy that when $\eta_{\mu\mu}$ is positive, sensitivities with and without scalar NSI closely overlap in the range around [-90°, 0°]. This region poses a challenge in definitively attributing CP sensitivity to scalar NSI effects.

In conclusion, the results emphasize that the presence of scalar NSIs can indeed impact the CP sensitivity measured at the DUNE far detector.

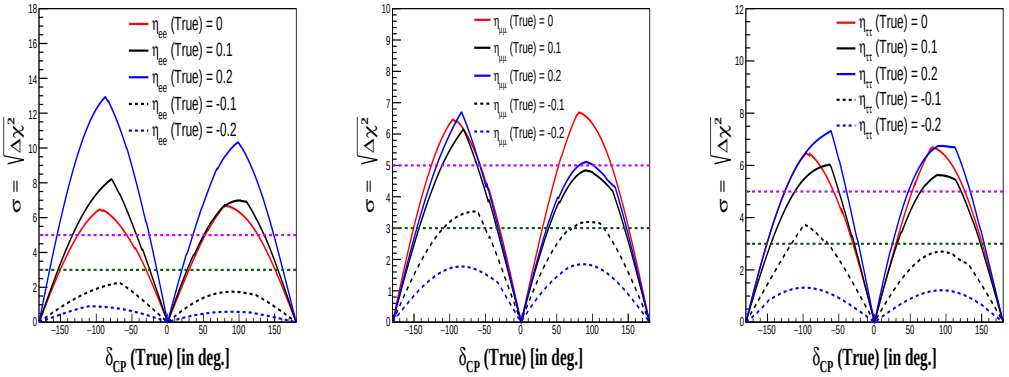

FIGURE 3.6: The CP-violation sensitivity of DUNE in presence of scalar NSI element $\eta_{\alpha\beta}$. The results for η_{ee} (top-left panel), $\eta_{\mu\mu}$ (top-right panel), and $\eta_{\tau\tau}$ (bottom panel) are shown. In all three plots, the red curve is for the 'no scalar NSI' case whereas the black and the blue solid (dashed) curves are for the chosen positive (negative) non-zero $\eta_{\alpha\beta}$.

3.4.4 Effects on the CP-precision measurements

Displayed within figure 3.7, we unveil the adeptness of DUNE to achieve precision in CP measurements when confronted with diagonal scalar NSI elements, namely η_{ee}, $\eta_{\mu\mu}$, and $\eta_{\tau\tau}$. This analytical endeavor encompasses the following steps Preservation of true mixing parameter values in a consistent manner. Implementation of marginalization over the test δ_{CP} and θ_{23} within their allowable ranges: [-π, π] and [40°, 50°], respectively. A specific value of δ_{CP}, set at -90°, is utilized. An additional marginalization is conducted over the test range of $\eta_{\alpha\beta}$, spanning -0.2 to 0.2. The representation takes shape as σ (expressing $\sqrt{\Delta\chi^2}$) plotted against varying test values of δ_{CP}. The graph incorporates magenta-dotted and green-dotted lines that correspond to $\Delta\chi^2$ values associated with 5σ and 3σ confidence levels, respectively. Through this comprehensive analysis, the

examination uncovers DUNE's precision potential in effectively constraining the test δ_{CP} values, relying on the known true values of δ_{CP}. We note that,

- Figure 3.7 (top-left panel) reveals an interesting trend where DUNE's capacity to constrain the δ_{CP} phase is enhanced (degraded) for positive (negative) non-zero η_{ee} values. In the absence of scalar NSI (the red curve), DUNE is expected to achieve a δ_{CP} precision of about -90°$^{+45°}$−48° at the 3σ confidence level. With scalar NSI, this precision can either improve or deteriorate. For instance, for ηee = 0.2, the precision enhances to -90°$^{+40°}$−30°. Conversely, for $\eta ee \leq$ -0.1, the CP-precision capability falls below the 5σ threshold.

- The top-right panel of figure 3.7 showcases the impact of $\eta_{\mu\mu}$ on DUNE's ability to constrain δ_{CP} values. For the 'no scalar NSI' scenario (red curve), DUNE's precision lies within $\sim$ -90°$^{+45°}$−48°. Notably, all non-zero negative $\eta\mu\mu$ values worsen the constraint on δ_{CP}, while a positive $\eta_{\mu\mu}$ marginally enhances it. For instance, with $\eta_{\mu\mu}$ = -0.2 (blue dashed line), the δ_{CP} precision falls below the 3σ level compared to the SI case.

- The bottom panel of figure 3.7 mirrors the pattern observed for η_{ee}, showcasing the analogous effect of $\eta_{\tau\tau}$ on CP-precision sensitivity. Notably, positive $\eta_{\tau\tau}$ values improve the precision capability, while negative $\eta_{\tau\tau}$ values reduce CP-precision sensitivity.

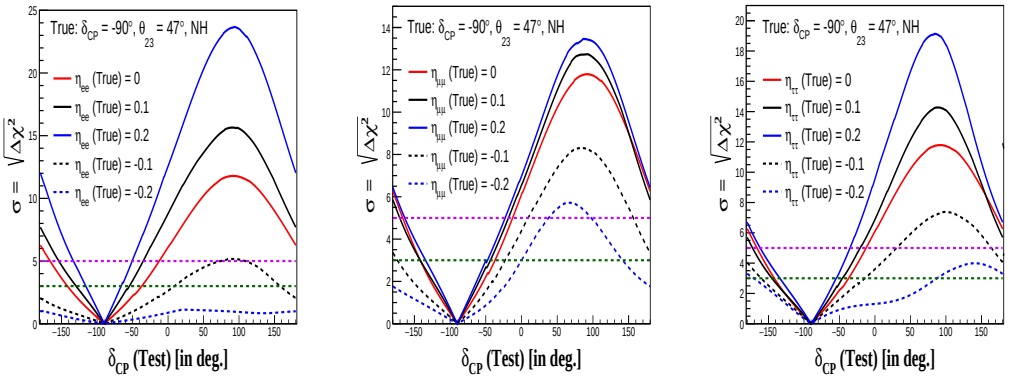

FIGURE 3.7: The CP-precision sensitivity in presence of $\eta_{\alpha\beta}$ for true δ_{CP} = -π/2 and true $\theta_{23} = 47°$. We show the results for η_{ee} (top-left panel), $\eta_{\mu\mu}$ (top-right panel) and $\eta_{\tau\tau}$ (bottom panel). In all the three plots, the red line is for the SI case.

3.5 Chapter Summary

In the realm of precision neutrino physics, the recognition of subtle effects such as Non-Standard Interactions (NSI) in neutrino experiments and their implications for the scientific potential of these experiments is of paramount importance. This study revolves primarily around DUNE, an exemplar Long-Baseline (LBL) candidate, to elucidate the ramifications of scalar NSI. Through a rigorous χ^2 analysis, we have delved into the impact of diagonal components within the scalar NSI matrix on the experiment. Notably, DUNE's sensitivity to $\eta_{\mu\mu}$ and $\eta_{\tau\tau}$ exhibits minimal disparity, albeit slightly favoring $\eta_{\mu\mu}$ with superior sensitivity. A nuanced observation emerges wherein the capability to constrain η_{ee} displays a modest decrease.

Our study further extends to comprehending the implications of scalar NSI on DUNE's CP-violation sensitivity. The infusion of scalar NSI is found to wield a significant influence on the experiment's CP sensitivity. For instance, a conceivable negative η_{ee} value, such as -0.10, pushes DUNE's CP sensitivity below the 3σ confidence level. On the flip side, positive non-zero η_{ee} values tend to augment DUNE's CP sensitivity compared to the 'no scalar NSI' scenario. Thus, given DUNE's exceptional accuracy and precision, the effects of scalar NSI cannot be discarded within the LBL framework.

Likewise, our CP-precision study unveils noteworthy outcomes. DUNE's ability to constrain the CP phase encounters substantial variation in the presence of scalar NSI. Positive $\eta_{\alpha\beta}$ elements predominantly enhance the experiment's prowess in gauging δ_{CP}, while negative $\eta_{\alpha\beta}$ elements tend to curtail this capacity. Evidently, constraining scalar NSI parameters is pivotal for accurate data interpretation across a spectrum of neutrino experiments. Additionally, the prospect of investigating scalar NSI within various neutrino mass models holds intrigue, as it directly interfaces with the neutrino Hamiltonian's mass component.